RESEARCH ARTICLE

WILEY

Cortical reorganization following auditory deprivation predicts cochlear implant performance in postlingually deaf adults

Zhe Sun[1] | Ji Won Seo[2] | Hong Ju Park[3] | Jee Yeon Lee[3] | Min Young Kwak[3] | Yehree Kim[3] | Je Yeon Lee[4] | Jun Woo Park[3] | Woo Seok Kang[3] | Joong Ho Ahn[3] | Jong Woo Chung[3] | Hosung Kim[1] ©

[1]USC Stevens Neuroimaging and Informatics Institute, Department of Neurology, Keck School of Medicine, University of Southern California, Los Angeles, California

[2]Department of Otorhinolaryngology-Head and Neck Surgery, Samsung Changwon Hospital, Sungkyunkwan University School of Medicine, Changwon, South Korea

[3]Department of Otorhinolaryngology-Head and Neck Surgery, Asan Medical Center, University of Ulsan College of Medicine, Seoul, South Korea

[4]Department of Otorhinolaryngology, Inje University Sanggye Paik Hospital, Seoul, South Korea

Correspondence
Hong Ju Park, Otorhinolaryngology-Head and Neck Surgery, Asan Medical Center, University of Ulsan College of Medicine, 88, Olympic-ro 43-gil, Songpa-gu, Seoul 05505, South Korea.
Email: dzness@amc.seoul.kr

Funding information
BrightFocus Foundation, Grant/Award Number: A2019052S; National Institute on Aging, Grant/Award Numbers: P41EB015922, U54EB020406

Abstract

Long-term hearing loss in postlingually deaf (PD) adults may lead to brain structural changes that affect the outcomes of cochlear implantation. We studied 94 PD patients who underwent cochlear implantation and 37 patients who were MRI-scanned within 2 weeks after the onset of sudden hearing loss and expected with minimal brain structural changes in relation to deafness. Compared with those with sudden hearing loss, we found lower gray matter (GM) probabilities in bilateral thalami, superior, middle, inferior temporal cortices as well as the central cortical regions corresponding to the movement and sensation of the lips, tongue, and larynx in the PD group. Among these brain areas, the GM in the middle temporal cortex showed negative correlation with disease duration, whereas the other areas displayed positive correlations. Left superior, middle temporal cortical, and bilateral thalamic GMs were the most accurate predictors of post-cochlear implantation word recognition scores (mean absolute error [MAE] = 10.1, r = .82), which was superior to clinical variables used (MAE: 12.1, p < .05). Using the combined brain morphological and clinical features, we achieved the best prediction of the outcome (MAE: 8.51, r = .90). Our findings suggest that the cross-modal plasticity allowing the superior temporal cortex and thalamus to process other modal sensory inputs reverses the initially lower volume when deafness becomes persistent. The middle temporal cortex processing higher-level language comprehension shows persistent negative correlations with disease duration, suggesting this area's association with degraded speech comprehensions due to long-term deafness. Morphological features combined with clinical variables might play a key role in predicting outcomes of cochlear implantation.

KEYWORDS

cochlear implant, hearing loss, plasticity, prognosis, voxel-based morphometry

- -

1 | INTRODUCTION

Hearing loss can affect health and quality of life. The worldwide prevalence of hearing loss is predicted to rise because of an aging population and increasing noise exposure. It was reported that nearly one in four individuals aged 12 years or older have hearing loss in at least one ear, and one in six have bilateral hearing loss in the United States (Goman & Lin, 2016). In postlingually deafened (PD) adults with severe and profound hearing loss who do not benefit from hearing aids, cochlear implantation (CI) is the only effective way to restore auditory function by bypassing the cochlea and stimulating the cochlear nerve directly (Cunningham & Tucci, 2017; Kral & O'Donoghue, 2010; Pacala & Yueh, 2012).

However, there is a large variation in speech performance in CI recipients and this variability in post-CI performance makes it difficult to provide appropriate and realistic counseling regarding the benefit of CI preoperatively. There are many factors that contribute to the variability including the cause of deafness, age at onset of deafness, duration of hearing deprivation, residual hearing, duration of hearing aid use, whether the better or poorer hearing ear receives the implant, and the CI technology (Beyea et al., 2016; Friedland, Venick, & Niparko, 2003; Holden et al., 2013; Lazard et al., 2012; Leung et al., 2005; Lin et al., 2012; Rubinstein et al., 1999). Another possible mechanism limiting post-CI speech performance after a period of auditory deprivation is cross-modal plasticity. It is widely accepted that deprivation of given sensory functions progressively results in shrinkage of the cortical representations (e.g., function or metabolism) of such nonused systems (Polley, Steinberg, & Merzenich, 2006; Steven & Blakemore, 2004). In PD adults, cross-modal plasticity is also observed to occur by the visual or somatosensory system recruiting the cortical regions that relate to the auditory information process (Fine, Finney, Boynton, & Dobkins, 2005; Finney, Clementz, Hickok, & Dobkins, 2003; Finney, Fine, & Dobkins, 2001; Kujala et al., 1997; Levanen & Hamdorf, 2001; Nishimura et al., 1999; Nishimura et al., 2000; Shibata, Kwok, Zhong, Shrier, & Numaguchi, 2001). Such cross-modal cortical changes may not be fully reversible even after original sensory function is recovered, likely explaining, at least in part, individually varying CI outcomes.

Neuroimaging studies also provide compelling evidence that the combined effects of the auditory function deprivation and the consequent cross-modal plasticity sophisticate the progression of cortical alterations (Lee et al., 2001; Lee et al., 2003). The temporal cortices show hypometabolism shortly after the onset of severe to profound hearing loss, and as the duration of the auditory deprivation extends, the metabolism is then observed to recover to the normal level as the temporal cortices participate in sensory functions other than auditory information processing (Lee et al., 2001; Lee et al., 2003; Lee et al., 2007). Furthermore, there is evidence that enhancement of visual input to the auditory cortex in long-term deafness might negatively impact the performance of CI (Collignon et al., 2011; Giraud & Lee, 2007).

Previous studies have focused on the association between the clinical features of PD patients (i.e., age at cochlear implantation, residual hearing, duration of deafness, and usage of hearing aid) and language

perception performance after CI, but prediction accuracy has been unsatisfactory (Peelle, Troiani, Grossman, & Wingfield, 2011; Stropahl, Chen, & Debener, 2017). The limited prediction of CI outcomes when using the clinical features might be improved by also quantitatively evaluating brain MRI features, which account for the cross-modal plasticity and the altered cortical structure and function that occurs in long-term deafness. To analyze multivariate clinical and imaging features, nonlinear fitting algorithms such as a random forest regression model may be more suitable than previously used correlation approaches because sophisticated and multidimensional patterns of cortical structural changes are required to be taken into account (Kim et al., 2018a). Furthermore, modeling of a machine learning-based regression using a training set and a validation set can build a computerized aiding system that allows for individualization of the prediction and may ultimately be able to assist clinicians in practice. Such approaches have been successfully used to improve disease diagnosis or predictions across various diseases (Ehteshami Bejnordi et al., 2017; Krittanawong, Zhang, Wang, Aydar, & Kitai, 2017; Moradi et al., 2015).

In this study, we aimed to investigate: (a) whether brain morphological changes in auditory and associated cortices are present in PD patients as compared with those who underwent brain MRI shortly after acute hearing loss, (b) how the brain gray matter probability changes in PD patients in relation to the duration of deafness, and (c) whether the comprehensive predictors as a combination of clinical features and imaging features that reflect brain structure can establish a robust individualized prediction model of word recognition abilities after CI in PD patients.

2 | METHODS

One hundred and thirty-seven participants were initially recruited in this study, including 98 postlingually deaf (PD) patients who underwent cochlear implantation (CI) and 39 patients who underwent sudden sensorineural hearing loss (SHL). After visually checking the image quality, six subjects (4 PD patients with CI and 2 patients with SHL) were identified with poor scan quality and subsequently excluded. Finally, 94 PD patients with CI and 37 SHL subjects remained for our analyses. These 94 bilateral deaf PD patients underwent CI with full electrode insertion in one ear which has worse hearing at Otology Clinic of Asan Medical Center from 2004 to 2015 and had audiological follow-up data for more than 2 years. Most of them (77/94) were implanted with CI devices from Cochlear Corp. (Lane Cove, New South Wales, Australia) with various types of electrodes and speech processors. Seventeen were implanted with devices from MED-EL (Innsbruck, Austria). They had various durations (range: 1–50 years; mean±SD: 16.6±15.5) of bilateral deafness which occurred after the acquisition of language skills. Thirty-seven age-matched SHL patients underwent brain magnetic resonance (MR) scans within 2 weeks after the onset of hearing loss. More specifically, the duration of hearing loss for SHL at MRI scan was 5.6 ± 3.4 days. These patients might not have significant brain structural changes but likely functional dynamic changes in relation to deafness. Thus, they were treated as controls

for the group comparison in the current study. Approval of the institutional review board at the host institute (Asan Medical Center) included a "waiver of consent" to allow sharing of data with collaborators without seeking further consent from participants because personal identifiers are not included in the data.

We used the following measurements as the prediction features of post-CI word recognition score (WRS): (a) duration of deafness (DoD), (b) age at CI surgery (ageCI), (c) duration of hearing aid use (DoHA), and (d) regional gray matter (GM) probabilities. DoD was determined by a review of available medical records. The duration of deafness was determined as the duration during which the patient reported little or no hearing in both ears before the CI operation. Some patients used hearing aids, though the benefit might have been minimal, and DoHA was defined as the duration of hearing aid use before the hearing aid became ineffective. As the definite cause of deafness in most of the patients was unknown, this factor was not included as a predictor in the analysis. In a previous study with 114 postlingually deaf adults, the mean rise time for the consonant–nucleus vowel–consonant (CNC) word scores to reach 90% of the CNC final score was 6.3 months (ranged 0.5–24 months), and most participants achieved this auditory improvement within the averaged time of all participants or even less (Holden et al., 2013). To best consider this, we assessed the CI performance after a minimum of 3 years after the cochlear implantation. The mean CI device duration used at the time of the latest language assessment was 183.21 ± 81.04 months (range, 40–352 months).

2.1 | Word recognition score as an outcome of CI

We used the scores of open-set monosyllabic word recognition tests in a quiet setting which is used for conventional speech audiometry as the outcome variables. Open-set speech perception tests were administered using 50 monosyllabic words in an audio-only condition: speech from a tester with the live voice at an $\sim$70 dB sound pressure level was presented 1 m in front of the patient. The tester could monitor whether the level of the speech volume of his/her speech is sufficiently loud during the test. In addition, the patients were required to repeat what they heard. The scores for correct keywords (out of 50) were presented as a percentage (%). The presenting sound pressure level was at speech reception threshold +40 dB or at the most comfortable level. Only the most recent audiologic evaluation was included in the post-CI analysis. Postoperative testing was conducted using the CI alone without the use of a hearing aid in the contralateral ear. The mean CI device duration used at the time of the latest language assessment was 183.21 ± 81.04 months (range, 40–352 months).

2.2 | Image acquisition

Presurgical MR imaging was performed using a 3T MRI scanner (Achieva; Philips Healthcare, the Netherlands) with an eight-channel coil. We acquired coronal T1-weighted turbo spin-echo images. T1-weighted imaging was performed with the following parameters: TR = 25 ms;

TE = 4.6 ms; FA = 30°; FOV = 180×180 mm^2; matrix = 300×300; voxel size = $0.6 \times 0.6 \times 0.6$ mm^3; thickness = 1.2 mm.

2.3 | Image processing

After acquiring the MR images, we corrected the radiofrequency field (B$_1$) inhomogeneity using nonparametric nonuniform intensity normalization (N3) algorithm (Sled, Zijdenbos, & Evans, 1998). We normalized the intensity range of the images into 0 to 100. After intensity normalization, we used FMRIB's Software Library (FSL), a software package developed at the Oxford Centre for Functional MRI of the Brain (http://fsl.fmrib.ox.ac.uk) which includes image analysis and statistical tools for the study of neuroimaging data (Bohland, Bokil, Allen, & Mitra, 2009). In this study, FSL version 5.0.9 was employed for the whole image analysis process including skull stripping, registration, and brain tissue segmentation. The details are described below:

To perform skull stripping and remove nonbrain parts, we used the Brain Extraction Tool (BET; ver 2.1). Skull stripping facilitated the subsequent image processing steps for image registration, and tissue segmentation. We then used the FSL-FLIRT tool to linearly register each image to the MNI-152 template in order to correct for the intracranial volume across subjects while normalizing the brain in the common space. These registered images were then classified into white matter (WM), gray matter, or cerebrospinal fluid (CSF) using FMRIB's Automated Segmentation Tool (FAST; ver 4.1), while also correcting for intensity nonuniformity. The segmentation routine implemented in the FAST toolbox was based on the hidden-Markov random field model and the associated expectation–maximization algorithm. The resulting outputs were the voxel-wise probability maps representing GM, WM, or CSF. We finally applied Gaussian smoothing to these maps with a kernel size of full width at half maximum (FWHM) of 5 mm. As a result, intensity of each voxel in the maps indicated a local weighted average generally expressed as GM, WM, or CSF concentration (= probability).

2.4 | Statistical analysis using voxel-based morphometry

SurfStat Toolkit was employed to perform statistical analyses using voxel-wise general linear models (GLMs) (Worsley, Wilson, Powe, & Benard, 2010). Details are delineated below:

2.5 | Group comparison

To identify brain areas where GM probabilities are different between the PD group and control group (i.e., patients with SHL), we used *group* as the independent variable in the linear model while including *sex* and *age at scan* as covariates in the analyses. We used a GM mask to restrict the analysis to the GM regions, which subsequently decreased the number of comparisons. We created this GM mask by averaging all the 137 individual GM probability maps and binarizing the average map by assigning

each voxel into either a background (0% GM probability) or a foreground (> 0%). To better localize findings with respect to the neocortex, we projected the significant voxels on to their nearest points on the cortical surface. The surface was extracted from the MNI-ICBM 152 template using CIVET-2.1.0 pipeline (http://www.bic.mni.mcgill.ca/ServicesSoftware/CIVET). Since the trend of cortical changes has not been decided, we performed group comparison using two-tailed Student's *t* test for both directions (PD > SHL and PD < SHL).

2.6 | Correlation of GM alterations with duration of postlingual deafness

To assess alterations in GM probability in relation to disease progression in the PD group, we constructed voxel-wise GLMs using the *age at scan*, *sex*, *DoD*, and *CI inserted site* (left or right) as variables. Then, we correlated the GM probability with DoD using the Pearson's correlation coefficient. Since the correlation direction was not hypothesized, we tested both positive and negative correlations.

We performed the correction for multiple comparisons using the random field theory (RFT) correction method at a $p < .05$ level of significance.

2.7 | Prediction of post-CI WRS with clinical and brain image features using random forest regression

2.7.1 | Statistical cluster-based approach

To build the feature clusters in the image space, we performed positive and negative correlations between WRS (a low score represents poor auditory language processing performance) and GM probability at each voxel within PD patients. This generated a collection of clusters demonstrating WRS-related spatial information without parcellation-derived boundaries, which might potentially avoid bias due to anatomical constraints. We created different sets of the clusters by generating the clusters at various t-value thresholds based on incremental thresholding on the t-value map generated from the correlation between WRS and GM probability (starting at $|t| = 0.05$, iteratively increasing by a small value as 0.05 until the maximum t-value observed in our data). The clusters resulted from each iteration were fed to a random forest regression (RFR) to separately regress the post-CI outcomes. To better evaluate the choice of a machine-learning model, we also tested the prediction of WRS using a support vector machine regression (SVMR) as a linear method.

2.7.2 | Parameter selection and validation strategy

Based on leave-one-out cross-validation and the minimization of the objective function using Bayesian optimization, we observed that the following parameters were used at the best performance: LSBoost as the ensemble-aggression method, number of learning cycles = 45, flag indicating to sample with replacement, and learning rate = 0.1.

3 | RESULTS

3.1 | Demographic characteristics

We acquired data from 94 PD patients (male: female = 37:57) and 37 SHL patients (male: female = 16:21). There was no significant
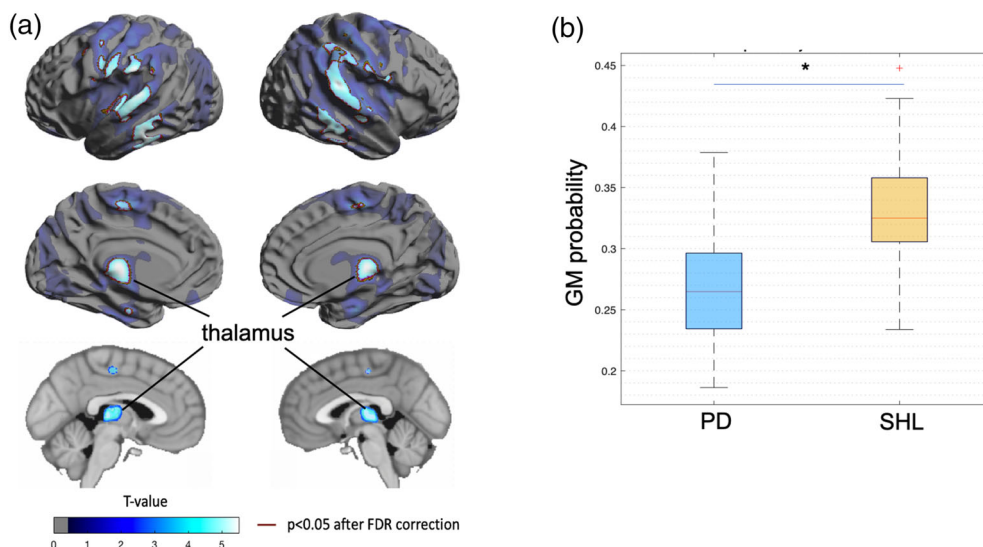

FIGURE 1 Gray matter (GM) probability in postlingually deafened patients. (a) Compared with the sudden hearing loss (SHL) controls, postlingually deafened patients presented lower GM probability in specific brain regions including the bilateral superior, middle and inferior temporal, supramarginal, and angular cortices as well as the primary motor and primary somatosensory cortical regions corresponding to the lips, tongue, and larynx. The significance was determined using false discovery rate (FDR) at 5%. (b) GM probabilities within the above-mentioned clusters of CI is significantly lower than that of SHL (*$p < .05$)

difference in age at scan between the PD group (51.66 ± 12.55) and the control group (48.73 ± 15.96, $p > .1$). In addition, the lateralization of the CI insertion was not significantly different between the PD group (right: left = 50:44) and the control group (right: left = 16:21, $p > .3$). The mean duration of deafness for the PD group was 15.77 ± 15.22 years and the mean duration of hearing aid use was 5.85 ± 7.83 years. The mean duration of deafness for the control group (patients with SHL) was only 8.5 weeks. The post-CI WRS of the PD group was checked from 4% to 96%, and the average was 66.02 ± 21.49%.

3.2 | Group comparison

Compared with the control group, the PD patients had significantly lower GM probability in specific brain regions including bilateral superior, middle, and inferior temporal cortices, supramarginal and angular cortices. The PD group also presented lower GM probability in the primary motor and primary

TABLE 1 Accuracy in random forest regression and support vector machine regression prediction using different feature-sets

	RFR (MAE, *r*-value)	SVMR (MAE, *r*-value)
Clinical features only	12.06, 0.71	13.71, 0.65
Imaging features only	10.14, 0.82	12.34, 0.72
Combined features	8.51, 0.90	11.39, 0.81

Abbreviations: MAE, mean absolute error, *r*-value: Pearson's correlation coefficient; RFR, random forest regression; SVMR, support vector machine regression.
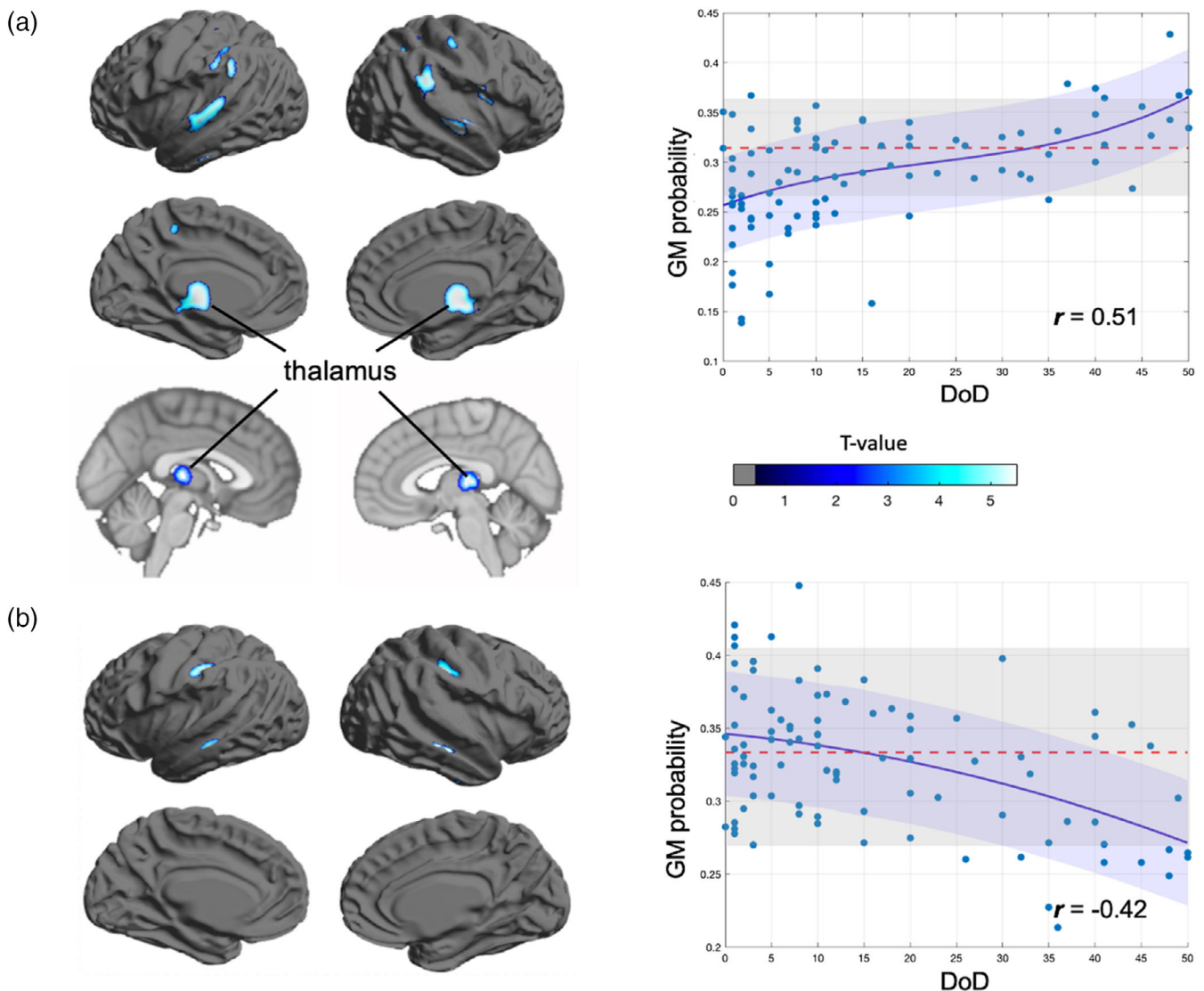

FIGURE 2 Association between duration of deafness (DoD) and gray matter (GM) probability. (a) GM probability increased with longer DoD in locations including the bilateral superior temporal cortices (STC), thalami and Wernicke's area as well as in small clusters located in right insular and posterior central cortices ($r = .51$). The significance was determined using false discovery rate (FDR) at 0.05. (b) GM probability decreased with longer DoD found in bilateral middle temporal and postcentral cortices ($r = .42$). The smallest standard errors were found with nonlinear fittings: the progressive GM increase was best fitted with a third order polynomial function whereas the progress GM decrease was fitted with a second order polynomial function. The red dotted lines and the gray transparent bands indicate the mean and 1 *SD* of the controls

somatosensory cortical regions corresponding to the movement and sensation of the lips, tongue, and larynx ($p < .05$ after FDR correction). The bilateral thalamus also had lower GM probability in PD patients. These results are shown in Figure 1.

3.3 | Relationship with the duration of deafness in postlingually deafened patients

The results of the voxel-wise correlation between the DoD and GM probability within PD patients are shown in Figure 2. Longer
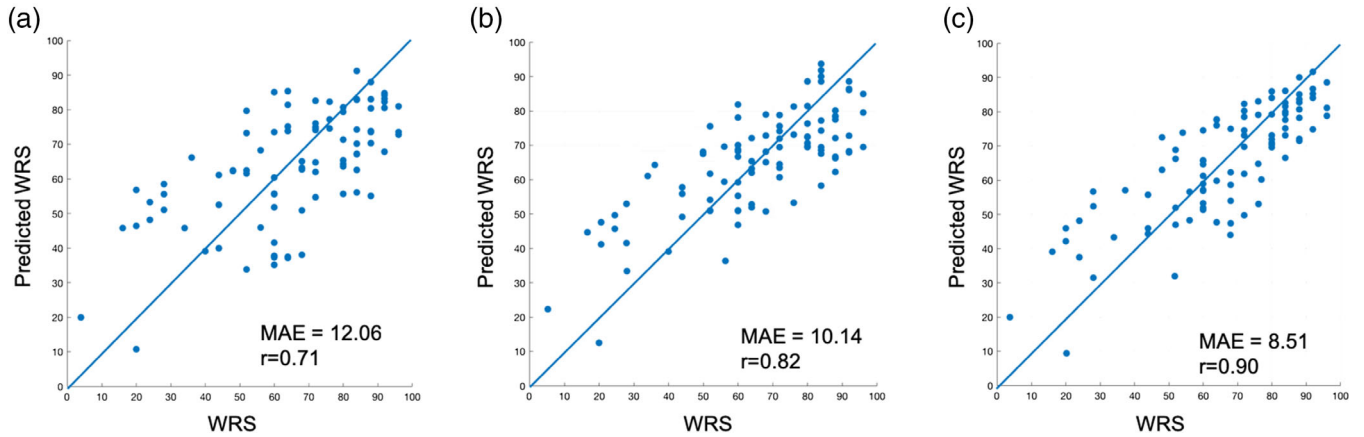

FIGURE 3 Post-CI WRS prediction using different feature-sets. (a) Prediction using clinical features only; (b) using neuroimaging features only; (c) using the combination of both feature-sets, generating the most accurate prediction result
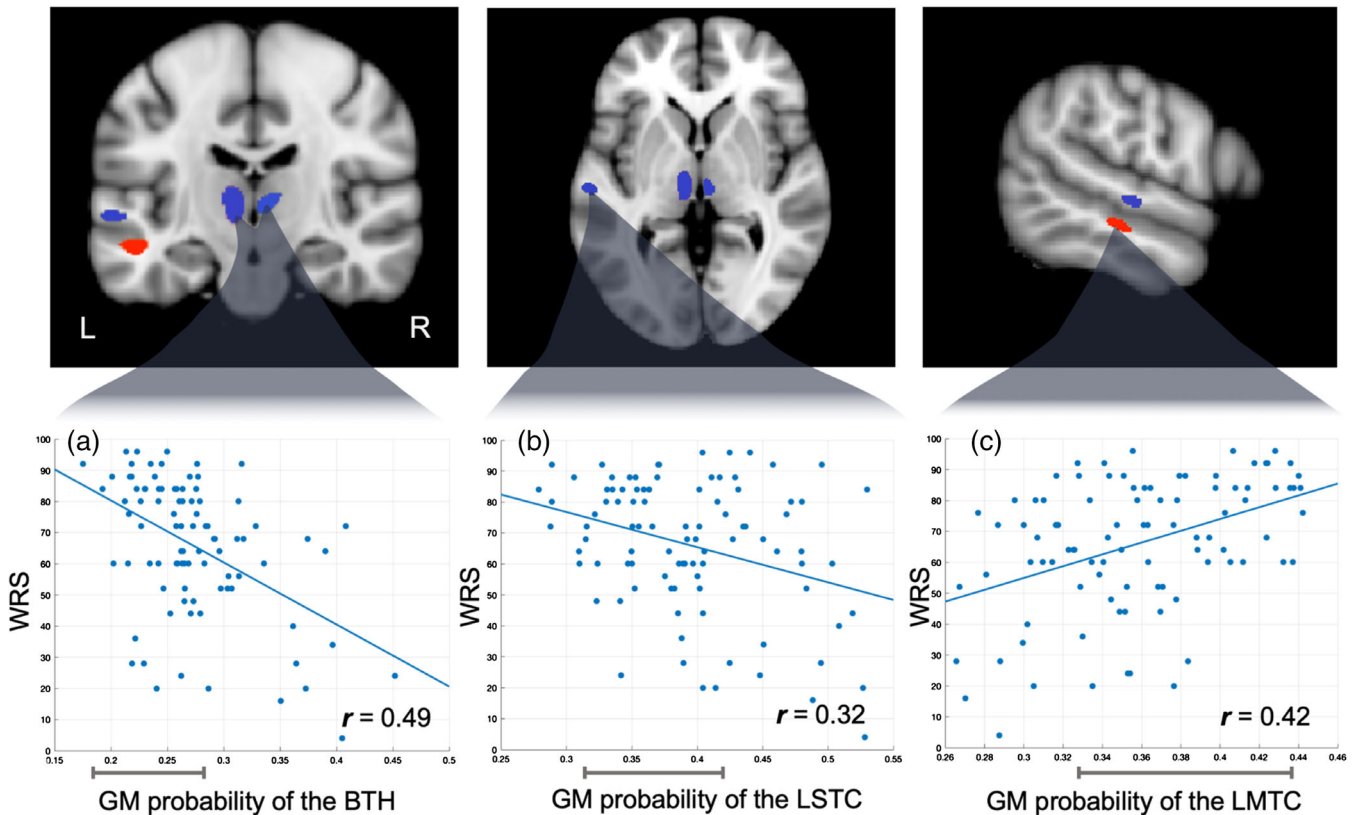

FIGURE 4 Prediction of post-cochlear implantation word recognition score (WRS) using the combined feature-sets. Clusters located in the bilateral thalami (BTH), the left superior temporal cortex (LSTC), and the left medial temporal cortex (LMTC) were found to contribute to the most accurate prediction result (MAE = 8.51 in Figure 3). (a) GM probability in each cluster located in the BTH and (b) the LSTC negatively correlates with WRS. (c) Each cluster located in the LMTC is positively correlated with WRS. The gray bars present the distribution (mean ± 1 *SD*) of controls

deafness duration was associated with higher GM probabilities in the bilateral superior temporal cortices (STC), thalami (TH), and Wernicke's area as well as in small clusters located in the right insular and posterior central cortices (Figure 2a; mean r = .51). On the other hand, longer deafness duration was also associated with lower GM probability in bilateral middle temporal cortices (MTCs; Figure 2b; mean r = .42). The patterns of GM probability changing along with deafness duration were likely nonlinear as higher order polynomial fitting curves best explained the patient distributions, yielding the lowest *SE* (positive association—third order polynomial, *SE* = 0.05; negative association—second order, *SE* = 0.04). The MTC-GM probability in PD with a longer duration (DoD > 10 years) significantly lower than that of control group (p = .02), whereas PD patients with a shorter duration (DoD ≤10 years) had no significant differences in GM probability compared with the control group (p = .9). The GM probability of bilateral STC in the deafness group with a shorter duration (DoD ≤10 years) was significantly lower than the control group (p < .0001), but GM probability in those with a longer duration (DoD > 10 years) did not differ from that in the control group (p = .9).

3.4 | Prediction of post-CI WRS using RFR and SVMR

The prediction accuracies of implementing an RFR model and a SVMR model based on each feature-set are summarized in Table 1. We used the mean absolute error (MAE), a measure of difference between observed values and predicted values (i.e., $\frac{\sum_{i=1}^{n} abs(y_i - x_i)}{n}$), to evaluate the model performance.

The RFR resulted in the MAE of 12.06 in prediction of the WRS using only clinical features (Table 1, Figure 3), meaning that the algorithm estimated the WRS for a test subject (which had not been included in training) to be close to the true WRS with an mean error of ±12.06 in word recognition score (range:0–100). Cluster-wise imaging features were observed to be better than clinical features, as the prediction using the imaging features was superior to that using the clinical features (MAE, 10.14 vs. 12.06; p < .05). After permutation, where various sizes of clusters were tested, the clusters contributing to the best prediction were located in the following four regions: left STC, left MTC and bilateral thalami (Figure 4 top). Correlation of the GM probabilities changes in the bilateral TH, left STC, and left MTC
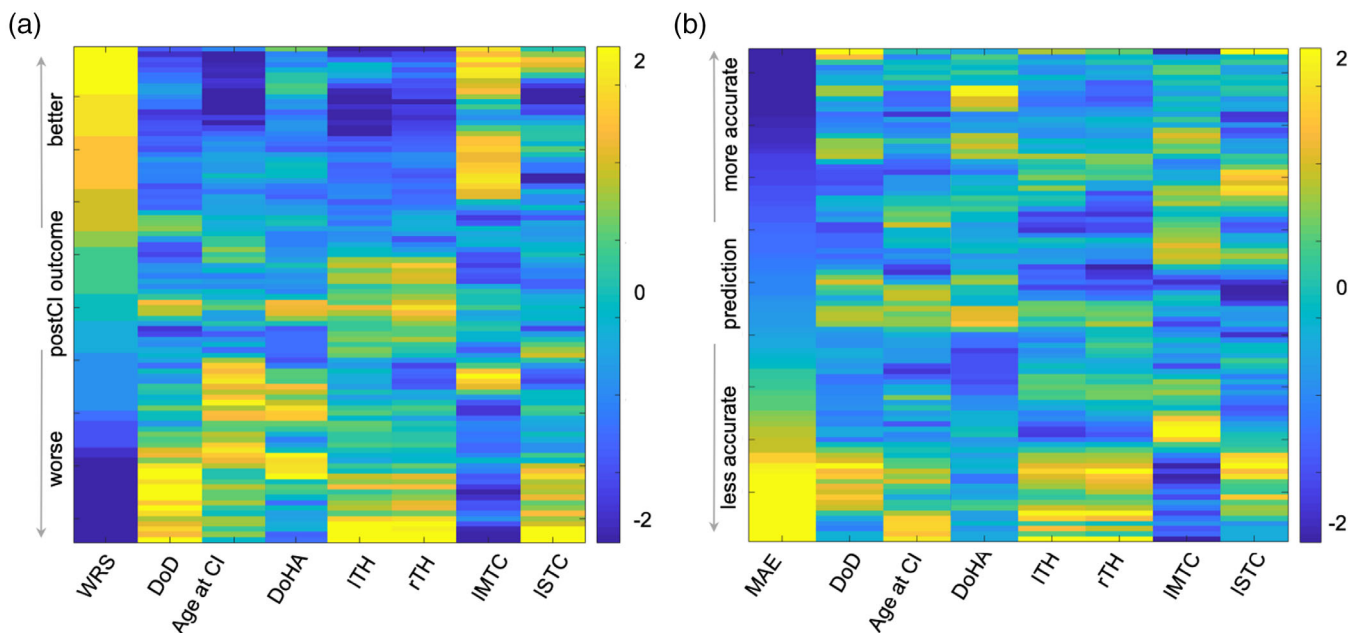

FIGURE 5 Heat mapping of the most accurate predictors. (a) Each postlingually deafened patient (n = 94) was first sorted separately by their postsurgical word recognition score (WRS); or (b) prediction accuracy (mean absolute error, MAE). The seven features (three clinical features and 4 MRI brain regional features) contributing to the most accurate prediction of post-cochlear implantation (CI) WRS are then normalized into a z-score and mapped on a cold-to-warm color scale. Each row represents an individual postlingually deafened patients. In panel a, the heat map shows the general tendency of each feature variation in relation to poor or good outcomes. For example, larger values for duration of deafness (DoD), Age at CI, DoHA, lTH, rTH, or lSTC is associated with a lower WRS (poor auditory language processing performance after CI), whereas a larger lMTC GM probability is associated with a higher WRS (good performance after CI). However, individual patterns show that a poor or good outcome could be explained, not solely by a specific feature, but by a combination of multiple features. The heat map in panel b displays feature variations in relation to prediction accuracy (MAE). Based on this map, the patients with less accurate prediction (high MAE) were those who consistently displayed a combination of a longer DoD, older at CI, larger GM in the left/right TH and left STC as well as smaller GM in the left MTC. MAE, mean absolute error; DoD, duration of deafness; CI, cochlear implant; DoHA, duration of use of hearing aid; lTH, left thalamus; rTH, right thalamus; lMTC, left middle temporal cortex; lSTC, left superior temporal cortex

with WRS showed significant association (Figure 4 bottom; r = −.49, −.32, and .42, respectively).

The clinical utility of the imaging features is based on our observation that the prediction of post-CI WRS for those with a long deafness duration (DoD > 10 years) showed lower prediction error against the prediction using the clinical features (MAE: 8.58 vs. 14.18) than for those with a short duration (DoD ≤10 years; MAE:10.42 vs. 13.54).

To evaluate the performance of RFR, we also predicted WRS using the linear SVMR method. Using different feature-sets, we observed that RFR models performed better than linear SVMR models (MAE decreased by 1.65–2.88; p < .05; Table 1).

Finally, we performed a heat mapping of individual features that contributed to the best prediction accuracy (MAE = 8.51) when combining clinical and imaging features and using them to validate an RFR model (Figure 5). Each individual PD patient (n = 94) was first sorted separately by their post-CI outcome (WRS) or prediction accuracy (MAE). The seven features (three clinical features and four MRI brain regional features) contributing to the most accurate prediction of post-CI WRS were then normalized into z-score and mapped on a cold-to-warm color scale. In Figure 5a, the heat map showed the general tendency of each feature variation in relation to poor or good outcomes. For example, a large value in DoD, Age at CI, DoHA, left and right TH and left STC are associated with a low WRS (poor auditory language processing performance after CI), whereas a large value in the left MTC GM probability is associated with a high WRS (good performance after CI). However, individual patterns showed that poor or good outcomes could not be explained solely by a specific feature, but by a combination of multiple features. The heat map in Figure 5b displays feature variations in relation to prediction accuracy (MAE). Based on this map, a patient with low values for left MTC and DoHA and large values for all other features was expected to achieve poor prediction accuracy (high MAE). The patients with less accurate prediction were those who consistently displayed a combination of a longer DoD, older at CI, larger GM in the left and right TH and left STC as well as smaller GM in the left MTC.

4 | DISCUSSION

In our cross-sectional design, the MR findings for the PD adults with various durations of bilateral deafness were compared with those of the control group. The underlying assumption was that the observed group differences would reflect cortical volume changes induced by bilateral deafness because the control group underwent a brain MR examination within 2 weeks after sudden hearing loss, which is a too short period for the brain cortex to exhibit marked structural changes compared with the changes due to long-term PD.

4.1 | GM volume decrease of auditory and associated cortices in postlingually deaf adults

In the current study, compared with the control group, patients with PD had significantly lower GM probabilities in bilateral superior,

middle, and inferior temporal cortices, as well as pre- and post-central cortices and bilateral thalami (p < .05). The locations showing such structural alterations have also been reported in previous studies where, after long-term postlingual deafness, alterations of metabolism in the associative auditory cortex and pre- and post-central cortices (Verger et al., 2017) as well as decrease in thalamo-auditory cortical projection (Chabot, Butler, & Lomber, 2015) were observed. Neural activities in the main auditory cortex (superior temporal), and lower auditory cortices (middle and inferior temporal) have been associated with speech comprehension in PD patients (Mortensen, Mirz, & Gjedde, 2006). Furthermore, MRI morphometry studies have reported that patients, even with mild to moderate hearing loss especially in the high frequency range, were associated with lower auditory cortex GM volume (Peelle et al., 2011; Stropahl et al., 2017). The pattern that we found in our group analysis is also confirmed by previous studies that the gray matter density and glucose metabolism in the primary auditory cortex of PD patients were lower than that in the normal hearing subjects (Han, Lee, Kang, Oh, & Lee, 2019; Kim et al., 2014). Compared with the control group, the PD patients also presented lower GM probability in the primary motor and primary somatosensory cortical regions corresponding to the movement and sensation of the lips, tongue, and larynx. Decreased auditory inputs have adverse effects on speech production, including articulatory decline and incapability of acquiring new vocabulary, which may indicate a link between sensory input and motor speech systems (Hickok & Poeppel, 2007). In our study, the sensorimotor cortical clusters displaying lower GM probability in the PD patients were mapped in the areas of parietotemporal boundary and premotor site that correspond to portions of the sensorimotor interface and articulatory network. This network has been hypothesized to be part of the dorsal auditory-sensorimotor integration circuit (Han et al., 2019). The presence of this network is also supported by a study using electroencephalography (EEG) and functional MRI, where cortical oscillations were observed in the transverse temporal area, somatosensory cortex, and the articulatory motor cortex at resting-state (Giraud & Poeppel, 2012). Therefore, the long-term auditory deprivation may lead to GM volume loss in the somatosensory and articulatory motor cortex as the result of compromise of auditory-sensorimotor integration circuit. This process potentially reflects a decrease in oral communication (= speech production) in deaf patients, which remains to be clarified. Altogether, these findings suggest that long-term hearing loss following onset of postlingual deafness leads to a systematic downregulation of neural activity during the processing of speech and may also contribute to cortical morphological changes such as decreases in GM volume.

4.2 | Progressive GM volume changes of auditory and associated cortices in deafness

Intriguingly, we found that the regions showing decreases in GM probability in PD patients compared with SHL controls undergo two distinctive trajectories of disease progression: longer deafness

duration was associated with higher GM probabilities in the bilateral STC, thalami, and Wernicke's area as well as in small clusters located in right insular and posterior central cortices, whereas longer deafness duration was associated with lower GM probability in bilateral middle temporal cortices.

The areas including the STC, thalamus, and Wernicke's area, as well as other small clusters that show progressive GM increases begin with significantly lower GM probabilities than controls. It has been shown that hearing loss leads to a systematic downregulation of neural activity in auditory and language cortical areas (Peelle et al., 2011; Stropahl et al., 2017). Hearing loss is also attributed to decreases in auditory cortical volume (Peelle et al., 2011). Therefore, the initial GM loss in the aforementioned areas may be associated with neural inactivity led by the lack of inquiry in auditory and language processing following hearing loss. However, the subsequent, progressive recovery of GM to the normal level in the auditory and language regions suggests a compensatory mechanism that operates through the reorganization of the plastic brain network to enable functional reallocation and more efficient processing of remaining modality sensory inputs (Alfandari et al., 2018). We speculate that after loss of auditory inputs, these brain regions undergo plastic cortical reorganization and are taken over by other sensory modalities, of which the most commonly seen is visual function (Strelnikov et al., 2013). Neural activities in the sensory regions that become strongly linked with these auditory-related regions through neuroplasticity and cortical reorganization mechanisms may continuously stimulate these brain regions, progressively resulting in their GM volume increase. More specifically, neural activity in the right angular gyrus is associated with the comprehension of degraded speech in the presence of visual speech cues. The greater volume in this area that was found in our study is in line with the reports of increased compensatory neural activity in the right-hemisphere networks at the presence of visual speech cues in long-term hearing loss patients (McGettigan et al., 2012; Pelson & Prather, 1974). Curve-fitting of GM probability in PD patients displays a pattern where the GM probability was positively associated with the deaf duration (shown in Figure 2a), reflecting the long-term nature of the compensatory brain reorganization. Furthermore, the progressive GM increase occurs even after recovery to the normal level, which invites further investigation.

We observed gradual decreases of the GM volume in the PD group in the middle temporal cortex (MTC) only. The role of MTC in long-term postlingual deafness remains unclear. In a diffusion tensor imaging study, the MTC was observed to connect with the Wernicke's area via the ventral auditory pathway (e.g., external capsule/uncinate fasciculus) (Parker et al., 2005). In contrast to the dorsal auditory pathway connecting the STC with the frontal premotor cortices, the ventral pathway mediates higher-level language comprehension (Saur et al., 2008). A transcranial magnetic stimulation study also confirms that areas of the MTG are involved in the retrieval of lexical syntactic information, a process required for high-order language comprehension. Therefore, the progressive GM loss found as a form of disrupted structural integrity in the MTC and may be associated with the degradation of speech comprehension in patients with long-term postlingual deafness.

4.3 | MR findings as factors predicting CI performances

With the advancement of cochlear implant (CI) technology, the majority of deaf individuals can at least partially regain their hearing abilities. However, large variation in the level of recovery due to the progression of cross-modal brain reorganization induced by hearing deprivation continues to present a challenge. Prediction of post-CI speech comprehension performance has relied on several preoperative clinical factors such as age at CI, duration of hearing loss, the presence of residual hearing, previous hearing aid use, and the presence of cochlear anomaly (Holden et al., 2013; Lazard et al., 2012; Leung et al., 2005). The duration of hearing loss has been considered to be the most substantial preoperative clinical factor for predicting post-CI outcome in PD patients (Blamey et al., 2013; Friedland et al., 2003; Holden et al., 2013; Lazard et al., 2012; Leung et al., 2005; Oh et al., 2003), but prediction of the performance in previous studies has been limited (Friedland et al., 2003; Roditi, Poissant, Bero, & Lee, 2009; Rubinstein et al., 1999). Our study using machine learning and heat mapping of clinical and imaging features shows that the brain cortical changes led by hearing deprivation do not always progress over time in a linear fashion. Analysis of the spatiotemporal pattern of cortical changes further shows that GM increases in the thalamus and STC are associated with poor post-CI speech comprehension, whereas GM increases in the MTC are associated with good outcomes. These findings collectively suggest the complex nature of brain reorganization, which is not necessarily fully characterized using preoperative clinical variables. As a result, our prediction model is most accurate when using the combined set of brain imaging and clinical features.

To the best of our knowledge, our study is the first observation in which structural changes in the primary auditory cortex and bilateral thalami are associated with post-CI performances in a large population of postlingually deaf patients. Moreover, we incorporated these findings into an individual prediction model of post-CI outcomes that may be useful in clinical practice. The importance of the brain structures that were found as predictors of the post-CI outcome is supported by previous functional imaging findings: the decreased auditory activations in the primary and association auditory cortices as well as the enhanced activation of the auditory cortex induced by visual stimulation in postlingually deaf patients are associated with poor post-CI speech comprehension (Green, Julyan, Hastings, & Ramsden, 2005; Sandmann et al., 2012; Stropahl et al., 2017). The medial geniculate nucleus, the GM probability of which was negatively correlated with post-CI outcomes in the current study, is part of the auditory thalamus and acts as the thalamic relay between the inferior colliculus and the auditory cortex. A previous study suggested that cross-modal plasticity activities generated in the auditory thalamus can also receive inputs from the superior colliculus, of which the upper layer receives visual signals from the retina (Bartlett, 2013). It is also noted that the use of hearing aid is associated with smaller volume in the left thalamus (Rudner et al., 2019). As smaller thalami and use of hearing aid (Kim et al., 2018b) are observed to associate with good CI outcomes,

this may indicate that use of hearing aid modulates the thalamic cognitive function or helps keep the integrity of the original function and structure, possibly leading to a higher success rate of CI.

The current study includes some limitations. There are recent reports that the auditory cortex may undergo volume loss (Fan et al., 2015) as well as functional reorganization (Campbell & Sharma, 2014) within the acute period of hearing loss. Such volume loss cannot be ruled out in our SHL controls and might have led to some of the observed difference in the GM probability between PD and control groups. However, as seen in Figures 2 and 3 in the study of Fan et al., the acute volume loss in relation to SHL was found only in a focal area of the auditory cortex contralateral to the site of hearing loss, whereas we found that the volume changes in relation to long-term PD were more widespread in multiple cortical areas including the auditory cortex. Thus, one might assume that the actual decrease of the auditory cortical volume in PD group was larger than that found in our study, due to possibly smaller auditory cortical volume of the SHL patients in this study than that of the normal hearing people. However, we have correlated GM probability with the duration of hearing loss in SHL patients (mean ± SD: 5 ± 3 days) and found no significant volume changes of auditory cortex within this relatively short period (vs. 9 ± 4 days in Fan et al.). With these collective findings, it is difficult to conclude that the use of SHL patients as controls affects our findings in the group comparison, However, future studies that use healthy adults without hearing loss as the control group may rule out the possible effects of using SHL controls and confirm our finding. Functional imaging studies show that the degree of neural activity in the occipital cortex in response to a visual stimulus is associated with deafness duration (Shiell, Champoux, & Zatorre, 2015) and post-CI outcome (Green et al., 2005; Sandmann et al., 2012; Strelnikov et al., 2013; Stropahl et al., 2017). However, we observed no structural changes in the visual cortex in the PD group in relation either to deafness progression or post-CI outcome, which is in accordance with other structural MRI studies (Peelle et al., 2011; Pereira-Jorge et al., 2018). This lack of a relationship between structure changes in the visual cortex and post-CI outcome needs further clarification but indicates that the neural activity in the original visual processing site may not exceed the normal range, thus inducing no structural alteration of the visual cortex in the context of cortical reorganization.

5 | CONCLUSIONS

Our findings suggest that postlingual deafness induces initial gray matter volume loss in the superior temporal cortex and thalamus, while the cross-modal plasticity that enables these regions to process other modal sensory inputs reverses the pattern of the volume decrease when deafness becomes persistent for years. However, volumes of the middle temporal cortex, which processes higher-level language comprehension, persistently decrease over time, suggesting this area's association with the degradation of speech comprehension in patients with long-term postlingual deafness. Pattern learning of gray matter density clusters in the left superior temporal cortex, left

middle temporal cortex, and bilateral thalami showed the most accurate prediction of post-cochlear implantation word recognition scores, which was slightly improved when combined with clinical variables like deafness duration and age at cochlear implantation. These imaging features of the cross-modal plasticity and progressive atrophy of language processing areas might play a key role in predicting outcomes of cochlear implantation.

AUTHOR CONTRIBUTIONS
Zhe Sun, Ji Won Seo: Manuscript drafting, data collection and analysis; Jee Yeon Lee, Min Young Kwak, Yehree Kim, Je Yeon Lee, Jun Woo Park: data collection and analysis; Hong Ju Park, Woo Seok Kang, Joong Ho Ahn, Jong Woo Chung, Hosung Kim: manuscript preparation, manuscript editing, data analysis, and interpretation. All authors reviewed and approved the manuscript.

ORCID
Hosung Kim ⓘ https://orcid.org/0000-0002-2269-8644

REFERENCES
Alfandari, D., Vriend, C., Heslenfeld, D. J., Versfeld, N. J., Kramer, S. E., & Zekveld, A. A. (2018). Brain volume differences associated with hearing impairment in adults. *Trends in Hearing*, *22*, 2331216518763689.

Bartlett, E. L. (2013). The organization and physiology of the auditory thalamus and its role in processing acoustic features important for speech perception. *Brain and Language*, *126*(1), 29–48.

Beyea, J. A., McMullen, K. P., Harris, M. S., Houston, D. M., Martin, J. M., Bolster, V. A., ... Moberly, A. C. (2016). Cochlear implants in adults: Effects of age and duration of deafness on speech recognition. *Otology & Neurotology*, *37*(9), 1238–1245.

Blamey, P., Artieres, F., Baskent, D., Bergeron, F., Beynon, A., Burke, E., ... Lazard, D. S. (2013). Factors affecting auditory performance of Post-linguistically deaf adults using Cochlear implants: An update with 2251 patients. *Audiology and Neuro-Otology*, *18*(1), 36–47.

Bohland, J. W., Bokil, H., Allen, C. B., & Mitra, P. P. (2009). The brain atlas concordance problem: Quantitative comparison of anatomical parcellations. *PLoS ONE*, *4*(9), e7200.

Campbell, J., & Sharma, A. (2014). Cross-modal re-organization in adults with early stage hearing loss. *PLoS ONE*, *9*(2), e90594–e90594.

Chabot, N., Butler, B. E., & Lomber, S. G. (2015). Differential modification of cortical and thalamic projections to cat primary auditory cortex following early- and late-onset deafness. *The Journal of Comparative Neurology*, *523*(15), 2297–2320.

Collignon, O., Champoux, F., Voss, P., & Lepore, F. (2011). Sensory rehabilitation in the plastic brain. *Progress in Brain Research*, *191*, 211–231.

Cunningham, L. L., & Tucci, D. L. (2017). Hearing loss in adults. *The New England Journal of Medicine*, *377*(25), 2465–2473.

Ehteshami Bejnordi, B., Veta, M., Johannes van Diest, P., van Ginneken, B., Karssemeijer, N., Litjens, G., ... Venâncio, R. (2017). Diagnostic assessment of deep learning algorithms for detection of lymph node metastases in women with breast cancer. *JAMA*, *318*(22), 2199–2210.

Fan, W., Zhang, W., Li, J., Zhao, X., Mella, G., Lei, P., ... Xu, H. (2015). Altered contralateral auditory cortical morphology in unilateral sudden sensorineural hearing loss. *Otology & Neurotology*, *36*(10), 1622–1627.

Fine, I., Finney, E. M., Boynton, G. M., & Dobkins, K. R. (2005). Comparing the effects of auditory deprivation and sign language within the auditory and visual cortex. *Journal of Cognitive Neuroscience*, *17*(10), 1621–1637.

Finney, E. M., Clementz, B. A., Hickok, G., & Dobkins, K. R. (2003). Visual stimuli activate auditory cortex in deaf subjects: Evidence from MEG. *NeuroReport*, *14*(11), 1425–1427.

Finney, E. M., Fine, I., & Dobkins, K. R. (2001). Visual stimuli activate auditory cortex in the deaf. *Nature Neuroscience*, *4*(12), 1171–1173.

Friedland, D. R., Venick, H. S., & Niparko, J. K. (2003). Choice of ear for cochlear implantation: The effect of history and residual hearing on predicted postoperative performance. *Otology & Neurotology*, *24*(4), 582–589.

Giraud, A. L., & Lee, H. J. (2007). Predicting cochlear implant outcome from brain organisation in the deaf. *Restorative Neurology and Neuroscience*, *25*(3–4), 381–390.

Giraud, A.-L., & Poeppel, D. (2012). Cortical oscillations and speech processing: Emerging computational principles and operations. *Nature Neuroscience*, *15*(4), 511–517.

Goman, A. M., & Lin, F. R. (2016). Prevalence of hearing loss by severity in the United States. *American Journal of Public Health*, *106*(10), 1820–1822.

Green, K. M., Julyan, P. J., Hastings, D. L., & Ramsden, R. T. (2005). Auditory cortical activation and speech perception in cochlear implant users: Effects of implant experience and duration of deafness. *Hearing Research*, *205*(1–2), 184–192.

Han, J. H., Lee, H. J., Kang, H., Oh, S. H., & Lee, D. S. (2019). Brain plasticity can predict the Cochlear implant outcome in adult-onset deafness. *Frontiers in Human Neuroscience*, *13*, 38.

Hickok, G., & Poeppel, D. (2007). The cortical organization of speech processing. *Nature Reviews. Neuroscience*, *8*(5), 393–402.

Holden, L. K., Finley, C. C., Firszt, J. B., Holden, T. A., Brenner, C., Potts, L. G., ... Skinner, M. W. (2013). Factors affecting open-set word recognition in adults with cochlear implants. *Ear and Hearing*, *34*(3), 342–360.

Kim, E., Kang, H., Lee, H., Lee, H. J., Suh, M. W., Song, J. J., ... Lee, D. S. (2014). Morphological brain network assessed using graph theory and network filtration in deaf adults. *Hearing Research*, *315*, 88–98.

Kim, H., Kang, W. S., Park, H. J., Lee, J. Y., Park, J. W., Kim, Y., ... Chung, J. W. (2018a). Cochlear implantation in Postlingually deaf adults is time-sensitive towards positive outcome: Prediction using advanced machine learning techniques. *Scientific Reports*, *8*(1), 18004.

Kral, A., & O'Donoghue, G. M. (2010). Profound deafness in childhood. *The New England Journal of Medicine*, *363*(15), 1438–1450.

Krittanawong, C., Zhang, H. J., Wang, Z., Aydar, M., & Kitai, T. (2017). Artificial Intelligence in Precision Cardiovascular Medicine. *Journal of the American College of Cardiology*, *69*(21), 2657–2664.

Kujala, T., Alho, K., Huotilainen, M., Ilmoniemi, R. J., Lehtokoski, A., Leinonen, A., ... Näätänen, R. (1997). Electrophysiological evidence for cross-modal plasticity in humans with early- and late-onset blindness. *Psychophysiology*, *34*(2), 213–216.

Lazard, D. S., Vincent, C., Venail, F., van de Heyning, P., Truy, E., Sterkers, O., ... Blamey, P. J. (2012). Pre-, per- and postoperative factors affecting performance of postlinguistically deaf adults using cochlear implants: A new conceptual model over time. *PLoS ONE*, *7*(11), e48739.

Lee, D. S., Lee, J. S., Oh, S. H., Kim, S. K., Kim, J. W., Chung, J. K., ... Kim, C. S. (2001). Cross-modal plasticity and cochlear implants. *Nature*, *409*(6817), 149–150.

Lee, H. J., Giraud, A. L., Kang, E., Oh, S. H., Kang, H., Kim, C. S., & Lee, D. S. (2007). Cortical activity at rest predicts cochlear implantation outcome. *Cerebral Cortex*, *17*(4), 909–917.

Lee, J. S., Lee, D. S., Oh, S. H., Kim, C. S., Kim, J. W., Hwang, C. H., ... Lee, M. C. (2003). PET evidence of neuroplasticity in adult auditory cortex of postlingual deafness. *Journal of Nuclear Medicine*, *44*(1439), 1435–1439.

Leung, J., Wang, N. Y., Yeagle, J. D., Chinnici, J., Bowditch, S., Francis, H. W., & Niparko, J. K. (2005). Predictive models for cochlear implantation in elderly candidates. *Archives of Otolaryngology – Head & Neck Surgery*, *131*(12), 1049–1054.

Levanen, S., & Hamdorf, D. (2001). Feeling vibrations: Enhanced tactile sensitivity in congenitally deaf humans. *Neuroscience Letters*, *301*(1), 75–77.

Lin, F. R., Chien, W. W., Li, L., Clarrett, D. M., Niparko, J. K., & Francis, H. W. (2012). Cochlear implantation in older adults. *Medicine (Baltimore)*, *91*(5), 229–241.

McGettigan, C., Faulkner, A., Altarelli, I., Obleser, J., Baverstock, H., & Scott, S. K. (2012). Speech comprehension aided by multiple modalities: Behavioural and neural interactions. *Neuropsychologia*, *50*(5), 762–776.

Moradi, E., Pepe, A., Gaser, C., Huttunen, H., Tohka, J., & Alzheimer's Disease Neuroimaging Initiative. (2015). Machine learning framework for early MRI-based Alzheimer's conversion prediction in MCI subjects. *NeuroImage*, *104*, 398–412.

Mortensen, M. V., Mirz, F., & Gjedde, A. (2006). Restored speech comprehension linked to activity in left inferior prefrontal and right temporal cortices in postlingual deafness. *NeuroImage*, *31*(2), 842–852.

Nishimura, H., Doi, K., Iwaki, T., Hashikawa, K., Oku, N., Teratani, T., ... Kubo, T. (2000). Neural plasticity detected in short- and long-term cochlear implant users using PET. *NeuroReport*, *11*(4), 811–815.

Nishimura, H., Hashikawa, K., Doi, K., Iwaki, T., Watanabe, Y., Kusuoka, H., ... Kubo, T. (1999). Sign language 'heard' in the auditory cortex. *Nature*, *397*(6715), 116.

Oh, S. H., Kim, C. S., Kang, E. J., Lee, D. S., Lee, H. J., Chang, S. O., ... Koo, J. W. (2003). Speech perception after cochlear implantation over a 4-year time period. *Acta Oto-Laryngologica*, *123*(2), 148–153.

Pacala, J. T., & Yueh, B. (2012). Hearing deficits in the older patient: "I didn't notice anything". *JAMA*, *307*(11), 1185–1194.

Parker, G. J., Luzzi, S., Alexander, D. C., Wheeler-Kingshott, C. A. M., Ciccarelli, O., & Lambon Ralph, M. A. (2005). Lateralization of ventral and dorsal auditory-language pathways in the human brain. *NeuroImage*, *24*(3), 656–666.

Peelle, J. E., Troiani, V., Grossman, M., & Wingfield, A. (2011). Hearing loss in older adults affects neural systems supporting speech comprehension. *The Journal of Neuroscience*, *31*(35), 12638–12643.

Pelson, R. O., & Prather, W. F. (1974). Effects of visual message-related cues, age, and hearing impairment on speech reading performance. *Journal of Speech and Hearing Research*, *17*(3), 518–525.

Pereira-Jorge, M. R., Andrade, K. C., Palhano-Fontes, F. X., Diniz, P. R. B., Sturzbecher, M., Santos, A. C., & Araujo, D. B. (2018). Anatomical and functional MRI changes after one year of auditory rehabilitation with hearing aids. *Neural Plasticity*, *2018*, 9303674.

Polley, D. B., Steinberg, E. E., & Merzenich, M. M. (2006). Perceptual learning directs auditory cortical map reorganization through top-down influences. *The Journal of Neuroscience*, *26*(18), 4970–4982.

Roditi, R. E., Poissant, S. F., Bero, E. M., & Lee, D. J. (2009). A predictive model of cochlear implant performance in postlingually deafened adults. *Otology & Neurotology*, *30*(4), 449–454.

Rubinstein, J. T., Parkinson, W. S., Tyler, R. S., & Gantz, B. J. (1999). Residual speech recognition and cochlear implant performance: Effects of implantation criteria. *The American Journal of Otology*, *20*(4), 445–452.

Rudner, M., Seeto, M., Keidser, G., Johnson, B., & Rönnberg, J. (2019). Poorer speech reception threshold in noise is associated with lower brain volume in auditory and cognitive processing regions. *Journal of Speech, Language, and Hearing Research*, *62*(4S), 1117–1130.

Sandmann, P., Dillier, N., Eichele, T., Meyer, M., Kegel, A., Pascual-Marqui, R. D., ... Debener, S. (2012). Visual activation of auditory cortex reflects maladaptive plasticity in cochlear implant users. *Brain*, *135*(2), 555–568.

Saur, D., Kreher, B. W., Schnell, S., Kummerer, D., Kellmeyer, P., Vry, M. S., ... Weiller, C. (2008). Ventral and dorsal pathways for language.

Proceedings of the National Academy of Sciences of the United States of America, 105(46), 18035–18040.

Shibata, D. K., Kwok, E., Zhong, J., Shrier, D., & Numaguchi, Y. (2001). Functional MR imaging of vision in the deaf. Academic Radiology, 8(7), 598–604.

Shiell, M. M., Champoux, F., & Zatorre, R. J. (2015). Reorganization of auditory cortex in early-deaf people: Functional connectivity and relationship to hearing aid use. Journal of Cognitive Neuroscience, 27(1), 150–163.

Sled, J. G., Zijdenbos, A. P., & Evans, A. C. (1998). A nonparametric method for automatic correction of intensity nonuniformity in MRI data. IEEE Transactions on Medical Imaging, 17(1), 87–97.

Steven, M. S., & Blakemore, C. (2004). Visual synaesthesia in the blind. Perception, 33(7), 855–868.

Strelnikov, K., Rouger, J., Demonet, J. F., Lagleyre, S., Fraysse, B., Deguine, O., & Barone, P. (2013). Visual activity predicts auditory recovery from deafness after adult cochlear implantation. Brain, 136 (Pt 12), 3682–3695.

Stropahl, M., Chen, L. C., & Debener, S. (2017). Cortical reorganization in postlingually deaf cochlear implant users: Intra-modal and cross-modal considerations. Hearing Research, 343, 128–137.

Verger, A., Roman, S., Chaudat, R. M., Felician, O., Ceccaldi, M., Didic, M., & Guedj, E. (2017). Changes of metabolism and functional connectivity in late-onset deafness: Evidence from cerebral (18)F-FDG-PET. Hearing Research, 353, 8–16.

Worsley, D. F., Wilson, D. C., Powe, J. E., & Benard, F. (2010). Impact of F-18 fluorodeoxyglucose positron emission tomography-computed tomography on oncologic patient management: First 2 years' experience at a single Canadian cancer center. Canadian Association of Radiologists Journal, 61(1), 13–18.